Light-induced kinetic effects in solids

Vladimir M. Shalaev
Department of Physics, New Mexico State University, Las Cruces, New Mexico 88003

Constantine Douketis, J. Todd Stuckless,* and Martin Moskovits
Chemistry Department, University of Toronto, Canada M5S 1A1
(Received 4 October 1995)

A theory of light-induced kinetic effects, currents and/or potential differences induced in a solid when it is irradiated by light, is developed. The combination of momentum-selective interband (or inter-subband-band) excitation and band-dependent kinetic properties causes kinetic anisotropy in the motion of particles (electrons and/or holes) in the solid. The selectivity originates from the Doppler effect and leads to unequal excitation of carriers moving with and against the direction of the wave vector of light. General relations describing these effects in an arbitrary solid within a two-band approximation are derived. In particular, the theory of the light-induced drift (LID) of electrons in metals arising from direct and indirect electron transitions is developed. LID reaches its maximum with excitation in the vicinity of the energy gap between two conduction bands. The spectral dependence of the resultant current is shown to be strongly asymmetrical at photon energies close to the energy gap with the direction of the carrier flow depending on the photon energy. Another light-induced kinetic effect results from the intensity gradient due to the strong attenuation of light as it passes into a metal which leads to a nonuniform spatial distribution of excited electrons, resulting in large diffusive flows of excited electrons and holes that propagate against each other. The different mobilities of the electrons and the holes result in a net light-induced diffusive flow. Experimental observation of LID of hot electrons via spatially asymmetric photoemission from rough films is presented. Additionally, a previously observed anomalous angular dependence in one-photon and two-photon electron emission from rough Ag films is explained in terms of LID.

I. INTRODUCTION

In the 1970s Grinberg *et al.*[1,2] showed that transitions between subbands in semiconductors can produce large radiation-induced currents. The corresponding macroscopic momentum is of the order of the typical momentum of electrons or holes rather than of the photon momentum. This means that under certain conditions radiation can produce a much stronger effect than radiation pressure. Grinberg *et al.* have dubbed this phenomenon the resonant photon-drag effect (RPDE). The RPDE occurs when the charge mobilities differ for excited and ground bands so that, under resonant conditions, the balance between the four radiation-induced partial currents is destroyed and a large net current arises. The four currents correspond to two excited electron flows moving in opposite directions and two hole flows that are also counterpropagating.[3] An effect similar to the RPDE effect, involving transitions between parallel subbands in quantum wells and dubbed light-induced drift (LID), was suggested by Dykhne *et al.*[4] The theory of LID was developed further by Grinberg and Luryi[5,6] and by Stockman *et al.*[7] and observed experimentally by Wieck *et al.*[8] in 1990. Skok and Shalagin[9] considered LID of electrons excited between the Landau subbands of a semiconductor in a magnetic field. This effect was observed by Kravchenko *et al.*[10] A theoretical treatment of the RPDE in transitions between magnetic subbands was also presented by Gurevich and Vinnikov.[11]

Light-induced drift can also occur in gases. This phenomenon was first suggested by Gel'mukhanov and Shalagin[12] in 1979 and was observed by Antsygin *et al.*[13] later in the same year. Following these pioneering studies many further theoretical[14–16] and experimental papers on LID in atomic (Woerdman and co-workers[17]) and molecular gases (Hermans and co-workers[18] and Chapovsky *et al.*[18,19]) appeared in the literature. In particular, Popov *et al.* studied drift induced by polychromatic[20] and pulsed-periodic[21] light excitation; two-photon-excited drift was considered in Ref. 22, and LID sound generation by pulsed excitation was studied by Shalaev and Yakhnin.[23]

Since the RPDE and the LID effects have basically the same underlying conceptual basis, the terms ''RPDE'' and ''LID'' are equally descriptive and we will use them interchangeably.

We briefly describe the essential elements of LID by considering first the more simple case of LID in gases. Consider monochromatic radiation of frequency ω, close to the frequency ω_0 of a transition between ground state 1 and excited state 2 of an atom. When the radiation interacts with the atomic gas the velocity distributions $f_2(\mathbf{v})$ and $f_1(\mathbf{v})$ of the excited and unexcited atoms become asymmetrical (that is, the velocity averaged over the distribution is not zero). The asymmetry is due to the fact that the radiation excites predominantly those atoms whose velocity $\mathbf{v}$ is such that the corresponding Doppler shift $\mathbf{q}\cdot\mathbf{v}$ ($\mathbf{q}$ is the incident radiation wave vector) of the radiation frequency cancels out the frequency detuning $\Omega=\omega-\omega_0$. Consequently, in each state there exist directed atomic motions characterized by two fluxes:

$$\mathbf{j}_1=\int \mathbf{v}f_1(\mathbf{v})d\mathbf{v}, \quad \mathbf{j}_2=\int \mathbf{v}f_2(\mathbf{v})d\mathbf{v}, \text{ where } d\mathbf{v}\equiv d^3v.$$

These fluxes are colinear with the wave vector $\mathbf{q}$, but directed oppositely, and equal in magnitude, so that the total macroscopic flux $\mathbf{J}=\mathbf{j}_1+\mathbf{j}_2=0$. A nonabsorbing buffer gas offers resistance to these fluxes. Since the kinetic cross sections of the excited and unexcited atoms are in general different, the forces resisting the fluxes of the excited and unexcited atoms are also different. A net force is, therefore, produced which is exerted by the buffer gas on the absorbing gas as a whole. This leads to a directed macroscopic motion of the absorbing gas, characterized by the flux $\mathbf{J}=\mathbf{j}_1+\mathbf{j}_2 \neq 0$. The buffer gas is acted upon by a force of the same magnitude but of opposite direction, producing an opposing flux. Thus, the combination of velocity-selective excitation and state-dependent kinetic properties causes the gas to be kinetically anisotropic and leads to the above transport effects.

Similar to LID in gases, LID of a degenerate two-dimensional electron gas (2DEG) in semiconductors can be produced.[4–10] The electron motion in a 2DEG is quantum confined along one direction. The confinement can be achieved either by applying a magnetic field[9–11] or by creating quantum wells[4–8] in semiconductor heterostructures. In both cases, the light induces velocity-selective transitions of electrons between two quantum well states and two Landau levels, respectively. Since the electron mobilities are, in general, different in the two states, LID of the electron gas as a whole occurs. In the case of a 2DEG, LID is maximum when the electron transitions occur between two parallel or quasiparallel subbands ($m_1 \approx m_2$), i.e., when the dispersion law of the particles is independent, or weakly dependent, on the internal states. In that case, the interband energy $E_2(\mathbf{k})-E_1(\mathbf{k})=\hbar\omega_0$ is a constant independent of the electron momentum $\mathbf{k}$, the relative width of the absorption band due to transitions between states 1 and 2 is small, and the corresponding resonance in the spectrum is sharp. Theoretical treatments of LID in a 2DEG in semiconductors are similar to those for LID of atomic gases and can be formulated in terms of a simple two-level system. In particular, the frequency dependence of the LID of electrons in semiconductors is the same as for gases, and LID changes its direction according to the sign of the frequency detuning $(\omega-\omega_0)$ from resonance. This is because the particles moving with the light absorb photons to the blue of the absorption contour center and those moving against the light absorb to the red of the center.

An interesting case of the RPDE resulting from transitions between the (nonparallel, $m_1 \neq m_2$) heavy-hole and the light-hole valence subbands in bulk p-type Ge was theoretically suggested by Grinberg and Udod.[2] The balance between the four partial currents is destroyed in this case because the momentum relaxation time for the light holes, moving oppositely to the incident radiation wave vector, is much smaller than that for holes moving along the wave vector. Such a strong difference in relaxation time can be achieved if the optical phonon energy $\hbar\omega_{\text{phon}}$ has a value such that only the light holes with $\mathbf{k}\cdot\mathbf{q}>0$ interact with optical phonons, leading to substantially shorter relaxation time for the holes. This kind of RPDE can be realized only at sufficiently low temperatures ($k_BT \ll \hbar\omega_{\text{phon}}$) and for the special case of excitation when $\hbar\omega_{\text{phon}}$ is larger than the energy of the nonequilibrium light holes moving with the incident radiation but smaller than the energy of the light holes moving against the radiation, in which case a significant enhancement of the PDE can be achieved. A similar resonance with interband optical transitions was considered in Refs. 24,25. It is clear, however, that this mechanism cannot be efficient for electron interband transitions induced by light in the visible range of the spectrum where the energy of the excited electrons is much larger than the optical phonon energy.

Another type of resonance in bulk p-type germanium occurs when the excitation of current carriers is selective with respect to their momentum and the temperature is sufficiently low to provide a sharp boundary in the distribution of holes at the Fermi energy E_F. If the energies of nonequilibrium holes moving against and with the light (E_1^- and E_1^+, respectively) are such that $E_1^- < E_F < E_1^+$, only the holes with $\mathbf{k}\cdot\mathbf{q}<\mathbf{0}$ will be involved in optical transitions, resulting in a large net current.[1,6] Near resonance the PDE current can be enhanced by almost three orders of magnitude.

The momentum relaxation rates in the theories of Refs. 1,2,5,6 was actually identified with the inverse lifetimes of the corresponding subbands; i.e., no distinction was made between population relaxation, polarization relaxation, and momentum relaxation.[26] In particular, the important mechanism of momentum relaxation due to quasielastic collisions with impurities, which does not affect the lifetime (as does phonon emission), was not taken into account in Refs. 1,2,5,6. These collisions play a significant role for LID in general[12,14,26] and, in particular, they are important for LID when interband transitions are excited in solids at large photon energy.

To summarize, LID in solids has, so far, been studied mostly for 2DEG's in semiconductors and, for the cases considered above, in bulk p-type Ge. LID experiments in these systems usually require infrared lasers and low temperatures.

It is possible to broaden the class of systems in which light-induced kinetic effects can be observed and applied. In particular, it is worth considering effects that originate through arbitrary interband transitions (including those which can be excited by light in the visible range) in semiconductors and in other solids.

In a recent paper[27] we extended the previous treatments of LID to include electrons in metals. In this case, the electron transitions occur between two conduction bands which can be nonparallel. In contrast to the case for subband transitions in semiconductors, the nonparallelism is always significant for interband transitions, even if $m_1=m_2$, since the edges of the conduction bands are typically located in different points of $\mathbf{k}$ space. Accordingly, the dispersion relations are significantly different for different electron bands. For example, in the perfectly-free-electron model $E_1(\mathbf{k})=(\hbar^2/2m)k^2, E_2(\mathbf{k})=(\hbar^2/2m)(\mathbf{G}\pm\mathbf{k})^2$ and, therefore, one finds that the interband energy $E_2(\mathbf{k})-E_1(\mathbf{k})=(\hbar^2/2m)(G^2\pm 2\mathbf{k}\cdot\mathbf{G})$ strongly depends on the electron momentum ($\pm\mathbf{G}$ are the reciprocal-lattice vectors which generate the second band). This brings up a significant difference between LID in metals and in 2DEG's (or gases). The width of an absorption contour associated with an interband transition is usually very large.

Nevertheless, the selectivity of electronic excitation with respect to the projection of the electron momentum (velocity) on the wave vector of the incident light occurs even in this case, the key points being the following: (1) Because of dispersion, the probability of interband electron transitions depends on the crystal momentum of the electron, i.e., on its velocity. (2) The frequency of light observed by electrons moving with and against the light propagation direction is different because of the Doppler shift. Consequently, electrons having different momenta are excited according to the direction of their momenta relative to that of the light. (3) The dependence of the interband transition probability on the frequency (and, because of the Doppler effect, on the electron momentum) can be very strong, especially near the band gap. The resulting asymmetry of excitation together with the difference in electron mobilities in the excited and ground bands leads ultimately to LID. It is also important that despite the nonparallel character of the electron bands the efficiency of the direct (vertical) interband excitation can be high enough since, in this case, two of the three momentum projections of the excited electrons can vary over a wide range.

Recently a number of interesting papers has appeared reporting on the photon drag effect (PDE). Keller[28] considered the PDE in a single-level metallic quantum well, and the observation of the photomagnetism of metals which is partly due to the PDE was reported by Gurevich *et al.*[29] Also an important contribution to surface current in metals due to the anisotropy of electron transitions induced by light in combination with diffuse reflection of the electrons at the surface was analyzed by Gurevich and Laiho.[30] (One can find more references to the earliest papers on PDE and related phenomena in Ref. 30).

In the present paper we develop a general approach for considering and understanding light-induced drift in solids. Its principle distinctive features are dependence on optical excitations, which are selective with respect to the particle momentum, and an internal state-dependent momentum relaxation. The theory is developed in Sec. II on the basis of the generalized Boltzmann kinetic equations. These equations take into account the light-induced perturbation of the equilibrium distribution. In Sec. III the theory of LID is further developed with an emphasis on light-induced kinetic effects resulting from interband transitions. We predict that these effects can be obtained experimentally in many cases at room temperature, using lasers generating coherent radiation in the near-infrared, visible, and ultraviolet range of the spectrum. A general formula describing the LID current in an arbitrary material is derived in Sect. III. Within the two-orthogonalized-plane-wave approximation, the theory is specific to materials with an energy gap; it is applicable particularly to metals and builds upon our preliminary results.[27] We consider the conditions for optimizing light-induced kinetic effects. A formula describing the spectral dependence of LID with excitation near the energy gap is derived and discussed. In Sec. IV, we consider effects due to indirect electron transitions. Light-induced diffusion flow (LIDF) resulting from a nonuniform intensity distribution due, for example, to attenuation is discussed Sec. V. Quantitative estimates are presented in Sec. VI. Two experimental observations[27] of the manifestation of LID in rough silver films are discussed in Sec. VII. Further discussion is presented in Sec. VIII where the relative magnitudes of light-induced kinetic effects in various materials such as metals, semimetals, and insulators are compared.

II. LIGHT-INDUCED KINETIC EFFECTS IN SOLIDS: ANALYSIS OF GENERALIZED BOLTZMANN KINETIC EQUATIONS

We begin by considering the action of a traveling wave on electrons and/or holes capable of absorbing the light through interband transitions in solids. Since the photon momentum is negligibly small compared to the electron momentum, only **k**-conserving interband transitions take place. These are known as direct or vertical transitions. (We neglect at this point electron transitions assisted by phonon absorption or emission; see Sec. VIII.) Thus, the photon momentum affects electron excitation primarily through the Doppler relation determining the group momentum of particles excited by photons. Additionally, the slight nonvertical nature of the excitation due to light pressure is also neglected. Under optimum conditions for LID, the macroscopic momentum of the electron drift is of the order of the particle momentum, $\sim\hbar k$, while the nonvertical character of the optical transition associated with light pressure produces corrections to LID which are smaller by a factor $\sim\hbar q/\hbar k\sim 10^{-3}-10^{-2}$.[4,12,14,27]

We consider two bands (1 and 2) with energies $E_1(\mathbf{k})$ and $E_2(\mathbf{k})$, respectively. The dynamics of a particle (charge e) interacting with field $\boldsymbol{\varepsilon}$ within the one-electron approximation is described by the following Boltzmann equation:

$$\left[\frac{\partial}{\partial t}+\mathbf{v}_{\mathbf{k}}\cdot\boldsymbol{\nabla}_{\mathbf{r}}+(e/\hbar)\boldsymbol{\varepsilon}\cdot\boldsymbol{\nabla}_{\mathbf{k}}\right]f(\mathbf{k})=S(\mathbf{k}), \tag{1}$$

where $f(\mathbf{k})$ is the particle distribution function which depends on velocity $\mathbf{v}_{\mathbf{k}}=\hbar^{-1}\nabla_{\mathbf{k}}E(\mathbf{k})$, position vector $\mathbf{r}$, and time t and $S(\mathbf{k})$ is the collision integral. The space and time evolution of excited particles $(i=2)$ is described by the generalized Boltzmann equation, which includes the term describing interband transitions induced by light of intensity I and characterized by an excitation cross section $\sigma(\omega',\mathbf{k})$,

$$\left[\frac{\partial}{\partial t}+\mathbf{v}_{\mathbf{k}}\cdot\boldsymbol{\nabla}_{\mathbf{r}}+(e/\hbar)\boldsymbol{\varepsilon}\cdot\boldsymbol{\nabla}_{\mathbf{k}}+\Gamma_2\right]f_2(\mathbf{k})$$

$$=S_2(\mathbf{k})+I\sigma(\omega',\mathbf{k})[f(\mathbf{k})-2f_2(\mathbf{k})]. \tag{2}$$

The particle distribution functions $f_i(\mathbf{k})$ and collision integrals $S_i(\mathbf{k})$ in the two bands, $i=1$ and $i=2$, satisfy the equalities

$$S(\mathbf{k})=S_1(\mathbf{k})+S_2(\mathbf{k}), \tag{3}$$

$$f(\mathbf{k})=f_1(\mathbf{k})+f_2(\mathbf{k}). \tag{4}$$

Excited states in band 2 decay to states within band 1 at a rate Γ_2. We will assume that all bands below band 1 are occupied so that no relaxation to states lower than those of band 1 takes place. The decay rate Γ_2 includes band-to-band $(2\rightarrow 1)$ spontaneous relaxation and relaxation due to inelastic collisions. Nonradiative decay to optical phonons is usually unimportant in cases such as ours when the photon en-

ergy is much larger than typical phonon energies. The collision integrals $S_i(\mathbf{k})$ in (1) and (2) can include, in principal, all possible collisions except those which result in the $2\rightarrow 1$ interband relaxation which are included in Γ_2. We assume, however, that the dominant momentum relaxation mechanism involves quasielastic collisions for which the collision-induced energy change is relatively small, so that $\Delta E \ll E, \hbar\omega$. (However, the change in momentum direction can be significant.) This is a realistic model, especially in cases where light particles are scattered by heavy particles such as impurities. These kinds of collisions are also the ones most likely to result in large differences in the scattering rates in the two bands and, therefore, in a large net current.[26] Additionally, the dominant contribution of the quasielastic collisions allows one to neglect the possible momentum dependence of Γ_2.

The quantity $\boldsymbol{\varepsilon}$ in (1) and (2) is the sum of the external field and the field due to the light-induced nonuniform redistribution of charged particles inside the sample. The efficiency of interband transitions induced by light of intensity I is characterized by an excitation cross section $\sigma(\omega',\mathbf{k})$ defined per unit photon energy. In $\sigma(\omega',\mathbf{k})$ we take into account the Doppler shift $\mathbf{q}\cdot\mathbf{v_k}$ of the radiation frequency $\omega' \equiv \omega - \mathbf{q}\cdot\mathbf{v_q}$. I and q are the local intensity and wave vector inside the sample.

If we assume that the light excites only a small fraction of the particles so that the departure from equilibrium is small and a linear approximation can be used, then $f_2 \ll f_1$ and, therefore, $f(\mathbf{k}) \approx f_1^{(0)}(\mathbf{k})$. The interband contribution to the imaginary part of the dielectric constant $\boldsymbol{\epsilon} = \boldsymbol{\epsilon}' + i\boldsymbol{\epsilon}''$ can, then, be approximated by

$$\boldsymbol{\epsilon}'' = \hbar c \int \sigma(\omega,\mathbf{k}) f_1^{(0)}(\mathbf{k}) d\mathbf{k}. \tag{5}$$

The conservation of the number of particles in a band requires that

$$\int S_i(\mathbf{k}) d\mathbf{k} = 0, \tag{6}$$

since quasielastic collisions described by S_i do not result in band-to-band relaxation.

The frictional force per unit volume acting on the particles in the ith band is defined by the expression

$$\mathbf{F}_i = m_i \int S_i(\mathbf{k}) \mathbf{v_k} d\mathbf{k}, \tag{7}$$

and the total force $\mathbf{F}$ acting on the particles consists of two partial forces, $\mathbf{F} = \mathbf{F}_1 + \mathbf{F}_2$, which refer to the scattering of particles in the upper and lower bands. Within the linear approximation, $\mathbf{F}_i \propto -\mathbf{u}_i$ where $\mathbf{u}_i$ is the macroscopic velocity of the particles in the ith band. Thus one can write

$$\mathbf{F}_i / m_i = -\nu_i \mathbf{j}_i / e, \tag{8}$$

where e is the particle charge and $\mathbf{j}_i$, the current per unit surface area in the ith band, is given by

$$\mathbf{j}_i = e \int \mathbf{v_k} f_i(\mathbf{k}) d\mathbf{k}, \tag{9}$$

and m_i and ν_i are the effective particle mass and the scattering rate in the ith band, respectively. The total particle current is given by the sum of the partial currents in the two bands,

$$\mathbf{J} = \mathbf{j}_1 + \mathbf{j}_2. \tag{10}$$

Using Eqs. (1) and (2), we will develop below a set of balance equations for the charge and momentum. With no externally applied voltage, $\boldsymbol{\varepsilon} = \boldsymbol{\varepsilon}^{(0)} + \nabla_{\mathbf{r}}\phi$ where $\boldsymbol{\varepsilon}^{(0)}$ is the external oscillating field and ϕ is the potential resulting from the light-induced modification of the equilibrium distribution of the carriers. The term $\propto \boldsymbol{\varepsilon}^{(0)}$ vanishes after averaging over a period of oscillation. Within the linear approximation, the nonequilibrium term $\nabla_{\mathbf{r}}\phi$ will be small, and the approximation $(e/\hbar)\boldsymbol{\varepsilon}\cdot\boldsymbol{\nabla}_{\mathbf{k}} f(\mathbf{k}) \approx (e/\hbar)\boldsymbol{\varepsilon}\cdot\boldsymbol{\nabla}_{\mathbf{k}} f^{(0)}(\mathbf{k})$ is valid. Integrating in (1) over $\mathbf{k}$ and taking into account the symmetry of the equilibrium distribution function, $f^{(0)}(\mathbf{k}) = f^{(0)}(-\mathbf{k})$, the integral of $\nabla_{\mathbf{k}} f^{(0)}(\mathbf{k})$ over $\mathbf{k}$ gives zero. We therefore conclude that the term proportional to $\boldsymbol{\varepsilon}$ can be neglected, and the continuity equation governing the total particle charge is recovered:

$$e\frac{\partial N}{\partial t} + \boldsymbol{\nabla}_{\mathbf{r}}\cdot\mathbf{J} = 0. \tag{11}$$

Here $N \equiv N(\mathbf{r}) = N_1(\mathbf{r}) + N_2(\mathbf{r})$ is the nonequilibrium, light-induced, particle concentration (the time derivative of the equilibrium density number is zero).

If the terms in (1) are multiplied by $\mathbf{v_k}$ and the integration over $\mathbf{k}$ is performed, the contribution of the term proportional to $\boldsymbol{\varepsilon}$ can no longer be neglected. However, the diffusive contribution $\int v_k^2 \nabla_{\mathbf{r}} f(\mathbf{k}) dk$ can be neglected in comparison with the field term $(e/\hbar)\varepsilon \int \mathbf{v_k}\cdot\boldsymbol{\nabla}_{\mathbf{k}} f(\mathbf{k}) d\mathbf{k}$, provided the scale of the spatial nonuniformity is much larger than the lattice constant. If $m_1 \neq m_2$, momentum conservation requires that the particle velocity changes when absorbing a photon so that $\mathbf{v}_{\mathbf{k}}^{(1)} m_1 = \mathbf{v}_{\mathbf{k}}^{(2)} m_2$. Taking this into account and using (7)–(10), one obtains the macroscopic momentum balance equation

$$\frac{\partial \mathbf{J}}{\partial t} + \nu_1 \sigma_c \nabla_{\mathbf{r}}\phi = \frac{\nu_1 m_1 - \nu_2 m_2}{m_1}\mathbf{j}_2 - \nu_1 \mathbf{J}, \tag{12}$$

where the potential difference ϕ is related to the nonequilibrium particle distribution by

$$\phi = e \int \frac{N(\mathbf{r}')}{|\mathbf{r}' - \mathbf{r}|} d\mathbf{r}'. \tag{13}$$

The particle conductivity σ_c in (12) is defined in the usual way: $\sigma_c = \frac{1}{3}\nu_1^{-1} e^2 \int v^2 \nabla_E f^{(0)}(k) d\mathbf{k}$. (For the sake of simplicity we assume that σ_c is a scalar.)

Note that, if there is no momentum-selective particle excitation (i.e., $\mathbf{j}_2 = 0$) or if excitation does not change the particle mobility (i.e., if $\nu_1 m_1 = \nu_2 m_2$), then Eq. (12) describes conventional electrical transport. A nonzero current $\mathbf{J}$ can then appear only when an external voltage is applied.

The source term for the current of the excited particles, $\mathbf{j}_2$, is the term in (2) proportional to $I\sigma(\omega',\mathbf{k})$. The contribution to $\mathbf{j}_2$ of the ''field'' term in (2), $\propto (e/\hbar)\boldsymbol{\varepsilon}\cdot\boldsymbol{\nabla}_{\mathbf{k}}$, appears as the response to the light-induced redistribution of charges

resulting from $\mathbf{j}_2$ and, accordingly, this gives a nonzero contribution to $\mathbf{j}_2$ only as a second- (or higher-) order perturbation. We will neglect this term. The diffusive term ($\propto \mathbf{v_k}\cdot\boldsymbol{\nabla}_\mathbf{r}$) can, in principle, contribute to LID in first order, provided there is a strong light intensity gradient in the sample. For the sake of simplicity we will neglect the diffusive term in (2) and ascribe a relatively small spatial dependence to the light intensity. (The effect resulting from a rapid attenuation of the light in the sample, LIDF, will be discussed in Sec. V). Thus, multiplying (2) by $\mathbf{v_k}$ and integrating over $\mathbf{k}$, in the linear approximation one obtains

$$\left[\frac{\partial}{\partial t}+\Gamma_2+\nu_2\right]\mathbf{j}_2 = Ie\int \mathbf{v_k}\sigma(\omega',\mathbf{k})f_1^{(0)}(\mathbf{k})d\mathbf{k}. \qquad (14)$$

It is clear from (14) that $\mathbf{j}_2\neq 0$ only if the excitation cross section $\sigma(\omega',\mathbf{k})$ has an asymmetrical dependence on the particle velocity $\mathbf{v_k}$. This requirement is fulfilled because the Doppler effect provides velocity-selective excitation.

From the expression for the total force $\mathbf{F}$,

$$e\mathbf{F} = -\nu_1 m_1\mathbf{j}_1-\nu_2 m_2\mathbf{j}_2=(\nu_1 m_1-\nu_2 m_2)\mathbf{j}_2-\nu_1 m_1\mathbf{J}, \qquad (15)$$

it follows that, if the radiation induces a current $\mathbf{j}_2$, the force $\mathbf{F}$ and the particle current $\mathbf{J}$ cannot simultaneously vanish provided that $m_1\nu_1\neq m_2\nu_2$. If the particle system was previously at equilibrium, then upon turning on the field $\mathbf{J}=0$ initially, but as the upper band becomes populated a current $\mathbf{j}_2$ is produced, and with it a nonzero force $\mathbf{F}$, which in turn produces the net current $\mathbf{J}$. After a certain time a steady-state flow of carriers is established in a closed circuit with

$$\mathbf{F}=0, \quad \mathbf{J}=\frac{\nu_1 m_1-\nu_2 m_2}{\nu_1 m_1}\mathbf{j}_2. \qquad (16)$$

With an open circuit a steady state potential difference is eventually established such that [see Eq. (12)]

$$\mathbf{J}=\mathbf{J}_{\mathrm{LID}}+\mathbf{J}_\phi=0, \quad \nabla_\mathbf{r}\phi=\frac{\nu_1 m_1-\nu_2 m_2}{\nu_1 m_1}\mathbf{j}_2/\sigma_c=\mathbf{J}_{\mathrm{LID}}/\sigma_c. \qquad (17)$$

In this case the LID current $\mathbf{J}_{\mathrm{LID}}$ is exactly compensated by the current $\mathbf{J}_\phi$ caused by the electrostatic potential difference resulting from the light-induced nonequilibrium distribution of particles in the sample.

If the entire system is considered to be composed of the particles and the lattice (including impurities), there will be no momentum or energy transfer from the radiation to the system (neglecting light pressure). The particle current results from the light-induced momentum exchange between particles and the lattice [see (7) and (12)] which also results in a decrease in the entropy of the system at the expense of an increase in the entropy of the light. The effect is to create a directed particle flow from an initially chaotic distribution while at the same time the initially directed light is scattered isotropically. Thus, LID results from the exchange of entropy between the light and the medium rather than from radiation pressure. And, in spite of the fact that the Doppler effect depends on the photon momentum $\mathbf{q}$, neither the average magnitude of the acquired particle momentum nor its sign have anything in common with the momentum of the absorbed photons. Likewise the force $\mathbf{F}$ acting on the particles and the equal and opposite force operating on the lattice are also due to the entropy transfer between photons and particles. In some sense the light acts as ''Maxwell's demon,'' selecting particles based on their velocities.

III. THEORY OF THE LIGHT-INDUCED DRIFT OF ELECTRONS

In the previous section we did not consider the kinetic equation for the off-diagonal elements of the density matrix; instead we used the corresponding cross section σ determined by those elements. In general, off-diagonal elements characterize the light-induced coherence (polarization) between quantum states within the two bands. The coherence relaxation rate Γ, which, in general, includes a contribution from the spontaneous and the collision-induced coherence decay, must be calculated on the basis of the specific form of the collision integral. We will restrict our treatment to the case of homogeneous broadening ($\Gamma\gg qv$) when the asymmetry in the excitation of electrons moving with and against the light is relatively small. The excitation cross section $\sigma(\omega',\mathbf{k})$ is given by

$$\sigma(\omega',\mathbf{k})\propto \mathrm{Im}\left[\frac{|V_{1,2}(\mathbf{k})|^2}{E_2(\mathbf{k})-E_1(\mathbf{k})-\hbar\omega'-i\Gamma}\right], \qquad (18)$$

which can be approximated for the case of homogeneous broadening by

$$\sigma(\omega',\mathbf{k})\approx\sigma(\omega,\mathbf{k})-\mathbf{q}\cdot\mathbf{v_k}\frac{\partial\sigma(\omega,\mathbf{k})}{\partial\omega}. \qquad (19)$$

Using (14), (16), and (19), the steady-state current becomes

$$\mathbf{J}_{\mathrm{LID}}=-\mathbf{q}\frac{\nu_1 m_1-\nu_2 m_2}{\nu_1 m_1}\frac{eI}{\Gamma_2+\nu_2}\frac{\partial}{\partial\omega}\int v_\mathbf{q}^2\sigma(\omega,\mathbf{k})f_1^{(0)}(\mathbf{k})d\mathbf{k}. \qquad (20)$$

Since $E\gg\hbar\Gamma$, the Lorentz factor in (18) can be replaced by a δ function, i.e., $\sigma(\omega,\mathbf{k})\propto\delta[E_2(\mathbf{k})-E_1(\mathbf{k})-\hbar\omega]$. Thus, the transitions between two bands are restricted to the surface of constant interband energy, $\theta(\mathbf{k})=E_2(\mathbf{k})-E_1(\mathbf{k})-\hbar\omega=0$.

Through the formula

$$\int v_\mathbf{q}^2\sigma(\omega,\mathbf{k})f_1^{(0)}(\mathbf{k})d\mathbf{k}=v_0^2\int\sigma(\omega,\mathbf{k})f_1^{(0)}(\mathbf{k})d\mathbf{k}, \qquad (21)$$

we define v_0 as a characteristic velocity projection on the wave vector which lies on the surface $\theta(\mathbf{k})$. Using (5) and (21) one may rewrite (20) as follows:

$$\mathbf{J}_{\mathrm{LID}}=-\frac{\mathbf{q}}{q}\frac{\nu_1 m_1-\nu_2 m_2}{\nu_1 m_1}(ev_0)\frac{qv_0}{\Gamma_2+\nu_2}\left[\frac{I}{\hbar c}\frac{\partial\epsilon''}{\partial\omega}\right], \qquad (22)$$

which is a general formula describing LID in an arbitrary solid. According to (22), the net electron current is directed along the wave vector, with or against the light depending on the values of the parameters in the equation. LID is observed only when the particle mobility is different in the two bands. Within the approximation used, the formula also contains the term $qv_0/(\Gamma_2+\nu_2)$, characterizing the (nonequilibrium)

electron mean free path in the upper band as a fraction of the light wavelength. When this parameter is small a moving particle will not feel the full effect of the wave properties of the light, leading to a decreased Doppler effect. The efficiency and selectivity of the excitation is determined in (22) by the derivative of the imaginary part of the dielectric function with respect to frequency.

Let us now make the general approach developed above more specific by assuming the nearly-free-electron model, which is applicable, for instance, to metals. If the band gap at the zone boundary is not small, one must take explicit account of the nonspherical nature of the energy surfaces. The dispersion relations for the conduction bands of metals are adequately described within the two-orthogonalized-plane-wave (2OPW) approximation by[31]

$$2E_{1,2}=\beta[(\mathbf{k}+\mathbf{G})^2+k^2]\mp\{\beta^2[(\mathbf{k}+\mathbf{G})^2-k^2]^2+4|V_G|^2\}^{1/2}, \tag{23}$$

where $\beta=(\hbar^2/2m)$, $\pm\mathbf{G}$ are the reciprocal-lattice vectors which generate the second band, and V_G is the Fourier component of the pseudopotential ($2|V_G|$ is the energy gap). The surface of constant interband energy is given by

$$\begin{aligned}\Theta(\mathbf{k})&=E_2(\mathbf{k})-E_1(\mathbf{k})-\hbar\omega'\\&=\beta(\pm 2\mathbf{k}\cdot\mathbf{G}+G^2)\\&\quad-[(\hbar\omega\mp qv_q)^2-4|V_G|^2]^{1/2}\\&=0,\end{aligned} \tag{24}$$

where v_q is the velocity projection on the wave vector $\mathbf{q}$. The minus and plus signs in $\pm\mathbf{k}\cdot\mathbf{G}$ correspond to the two opposite directions of the reciprocal-lattice vector $\mathbf{G}$, and the minus and plus in ω' correspond to electrons moving with and against the light, respectively. If the wave vector $\mathbf{q}$ is assumed to be parallel to the vector $\mathbf{G}$, then expending (24) in terms of a small parameter qv_q, one can see that the surfaces of constant interband energy are planes that lie parallel to the zone boundaries (see Fig. 1). The crucial point is that the distances of the planes are not equal with respect to the origin of momentum space, $\mathbf{k}=0$, owing to the Doppler effect. As a result, when the system is illuminated, causing a slight increase (decrease) in the population in the upper (lower) bands, this process will be unequal for electrons traveling with and against the wave vector $\mathbf{q}$ since they involve electrons of somewhat different momenta.

The geometry of the planes given by (24) in the limit of small $\mathbf{q}\cdot\mathbf{v_q}$ and the surfaces $E_1=E$ and $E_2=E+\hbar\omega'$ are presented schematically in Fig. 1. Electron excitation takes place within an energy interval $E_{\min}<E<E_F$, where E_F is the nearly-free-electron Fermi energy. The low-energy cutoff $E_{\min}$, corresponding to the points c and c' in Fig. 1 and assuming $\hbar qv_{\mathbf{k}}\ll E_{\min}$, is given by[32]

$$E_{\min}=\frac{1}{2}mv_0^2=\frac{(\hbar\omega-\beta G^2)^2-4|V_G|^2}{4\beta G^2}. \tag{25}$$

According to Fig. 1, all electrons which can be excited by radiation have the same velocity projection on $\mathbf{q}$. Thus v_0 defined by (21) has the simple form in this case given by (25).

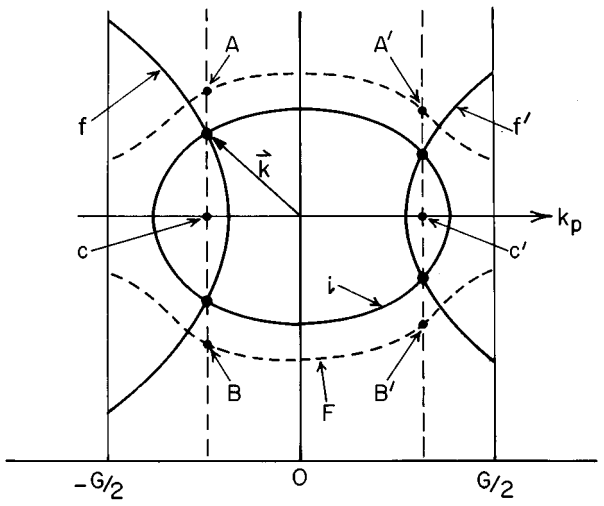

FIG. 1. Geometry of the constant energy surfaces for optical transitions at photon energy $\hbar\omega$ in the 2OPW approximation. $\mathbf{G}$ is the reciprocal-lattice vector which generates the second band; $k_p\equiv k_\parallel$ is the momentum projection on $\mathbf{G}$. F indicates the Fermi surface; point c (or c') defines $E_{\min}$ (see the text). The vertical dashed lines represent the planes of constant interband energy and the curves labeled i and f (or f') indicate the surfaces $E=E_i\equiv E_1$ and $E_f\equiv E_2=E+\hbar\omega$ which correspond to initial (i) and final (f) states, respectively. Direct transitions are permitted only for states lying on the disks whose diameters are represented by AB and $A'B'$. The asymmetry in the disks location with respect to the origin of momentum space is due to the Doppler effect.

The imaginary part of the dielectric constant ϵ'' has the form[32]

$$\epsilon''=\frac{2e^2}{3\hbar^4\omega^4}\frac{n_G G|V_G|^2}{1-\gamma}(E_F-E_{\min}), \tag{26}$$

where

$$\gamma=1-\left\{1-\frac{4|V_G|^2}{(\hbar\omega)^2}\right\}^{1/2}, \tag{27}$$

and n_G is the number of physically equivalent planes G. Using (22) and (25)–(27), one obtains the following expression for the steady LID current in metals:

$$\begin{aligned}\mathbf{J}_{\mathrm{LID}}=&-\frac{\mathbf{q}}{q}\frac{\nu_1 m_1-\nu_2 m_2}{\nu_1 m_1}(ev_0)\frac{qv_0}{E_F/\hbar-E_{\min}/\hbar}\\&\times\left[\frac{\Gamma_2}{\Gamma_2+\nu_2}\frac{I\epsilon''}{c\hbar\Gamma_2}\right]\Phi(\omega),\end{aligned} \tag{28}$$

where the spectral function $\Phi(\omega)$ is defined by

$$\Phi(\omega)=4\frac{E_F-E_{\min}}{\hbar\omega}\left[1+\frac{|V_G|^2}{(\hbar\omega)^2-4|V_G|^2}\right]+\frac{1}{2}\left(\frac{\hbar\omega}{E_G}-1\right). \tag{29}$$

The physical meaning of formula (28) may be clarified as follows. At steady state the concentration of excited electrons, N_2, is given by $N_2=(I\epsilon'')/(\hbar c\Gamma_2)$. The nonequilibrium distribution of the excited electrons will decay with a rate Γ_2 due to the interband relaxation and with rate ν_2 due

to quasielastic collisions, ultimately resulting in the equilibration of the excited states. The ratio $\Gamma_2/(\Gamma_2+\nu_2)$ expresses the fraction of excited electrons which remain in a nonequilibrium state and therefore contribute to the current. Accordingly, the term in square brackets in (28) represents the number density of excited nonequilibrium electrons. The term $(qv_0)/[E_F/\hbar - E_{\min}/\hbar]$ characterizes the selectivity of excitation with respect to electrons moving with and against the light. Formulas (28) and (29) are valid only for $(\hbar\omega - 2|V_G|) \gg \hbar\Gamma \gg kv_0$ and accordingly the selectivity term is small within this approximation.

When $(\hbar\omega - 2|V_G|) \to \hbar\Gamma$ the LID increases dramatically because the selectivity of the excitation with respect to counterpropagating electrons is significantly improved in this case. In order to calculate the efficiency of the excitation in the threshold region one needs to take into account the modification of ϵ'' due to the relaxation processes. In the constant matrix element approximation, ϵ'' is given by[32]

$$\epsilon'' = \frac{e^2 n_G G^2 |V_G|^2}{3\pi m^2 \omega^4} \int' d\mathbf{k}\,\delta(\Theta(\mathbf{k})), \tag{30}$$

where the prime on the integral denotes that the integration is to be performed only over those portions of **k** space for which $E_2 > E_F > E_1$. [Formula (26) follows from (30) when integrating over **k**.] Hereafter we assume that the thermal energy $k_B T$ is much less than any of the other energy parameters involved in the problem. Accordingly, the Fermi-Dirac distribution $f_1^{(0)}$ can be approximated by a step function.

First, we integrate in (30) over $d^2k_\perp$, the momentum projections which are perpendicular to the reciprocal-lattice vector **G**. Then, in the remaining integration over $dk_\parallel$, the momentum projections parallel to **G**, we express $k_\parallel$ in terms of $\xi \equiv E_1 - E_2$ using Eq. (23), and obtain

$$\epsilon'' = \epsilon_0'' \int_{-\infty}^{\infty} d\xi \frac{\xi}{\sqrt{\xi^2 - 4|V_G|^2}}\,\delta(\xi - \hbar\omega), \tag{31}$$

where

$$\epsilon_0'' = \frac{2e^2 n_G G |V_G|^2}{3\hbar^4 \omega^4}(E_F - E_{\min})$$

is the imaginary part of the dielectric function ϵ'' when $\hbar\omega \gg 2|V_G|$, i.e., when $\gamma \approx 0$ [see Eqs. (26) and (27)]. The integration in (31) gives formulas (26) and (27).

In the first approximation, the relaxation processes can be easily taken into account if the δ function in Eq. (31) is replaced by the Lorentzian $(\hbar\Gamma/\pi)[\xi^2 + (\hbar\Gamma)^2]^{-1}$. Performing the integration, we obtain

$$\epsilon'' = \epsilon_0'' R(\hbar\omega), \tag{32}$$

where the relaxation function $R(x)$ is defined as

$$R(x) = \frac{x/\sqrt{2}}{[(x^2 - x_0^2)^2 + 4\gamma_0^2 x^2]^{1/4}} \times \left(1 + \frac{x^2 - x_0^0}{[(x^2 - x_0^2)^2 + 4\gamma_0^2 x^2]^{1/2}}\right)^{1/2},$$

Hereafter, we use the notation $x \equiv \hbar\omega, x_0 \equiv 2|V_G|, \gamma_0 \equiv \hbar\Gamma$ [γ_0 should not be confused with γ in Eq. (27)].

In the limit $(\hbar\omega - 2|V_G|) \gg \hbar\Gamma$ formula (32) converts to (26) and (27). The function $R(x)$ in (32) has the strongest dependence on ω and its contribution to $\partial\epsilon''/\partial\omega$ in (22) is, therefore, the largest. (Thus, in the vicinity of the energy gap, we neglect the term $\propto \partial\epsilon_0''/\partial\omega$.) Substituting (32) to (22), one obtains

$$\mathbf{J}_{\mathrm{LID}} = \frac{\mathbf{q}}{q}\,\frac{\nu_1 m_1 - \nu_2 m_2}{\nu_1 m_1}(ev_0)\frac{qv_0}{\Gamma}\left[\frac{\Gamma_2}{\Gamma_2 + \nu_2}\,\frac{I\epsilon_0''}{c\hbar\Gamma_2}\right]L(\hbar\omega), \tag{33}$$

where

$$L(x) = R(x)\,\frac{\gamma_0^2 x_0^2}{(x^2 - x_0^2)^2 + 4\gamma_0^2 x^2}\left[\frac{x^2 - x_0^2}{\gamma_0 x} - \left(1 + \frac{x^2}{x_0^2}\right)\frac{2\gamma_0 x}{[(x^2 - x_0^2)^2 + 4\gamma_0^2 x^2]^{1/2} + x^2 - x_0^2}\right]. \tag{34}$$

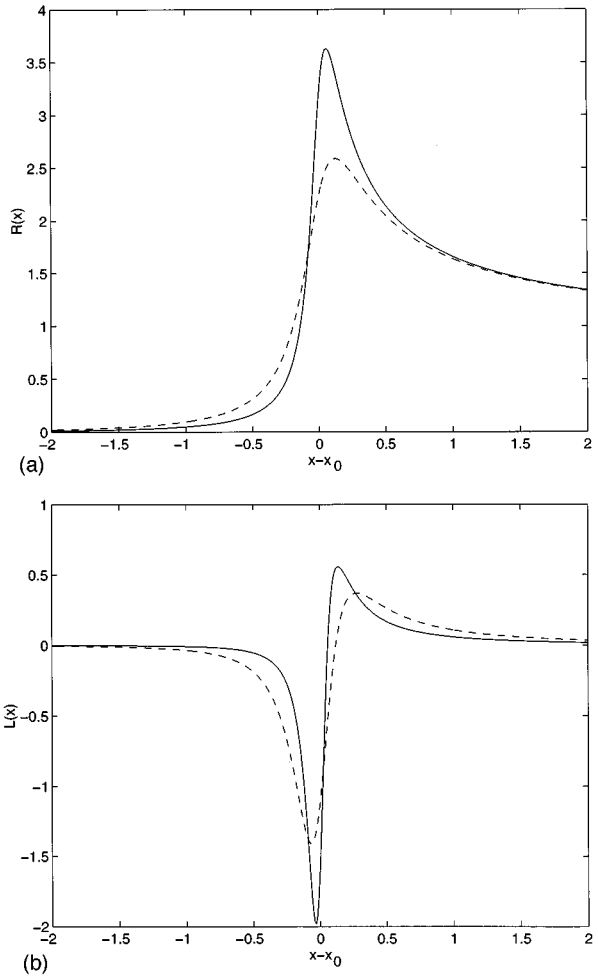

FIG. 2. Relaxation function $R(x)$ (a) and LID spectral function $L(x)$ (b) for $\hbar\Gamma = 0.1$ eV (solid lines) and $\hbar\Gamma = 0.2$ eV (dashed lines) at $2|V_G| \equiv x_0 = 4$ eV ($x \equiv \hbar\omega$). The function $L(\hbar\omega)$ ($\propto dR/d\omega$) describes the frequency dependence of LID excited in the vicinity of the energy gap.

Comparing (33) with (28) one can see that the selectivity parameter kv_0/Γ in (33) is significantly larger than its counterpart $(qv_0)/[E_F/\hbar - E_{\min}/\hbar]$, in (28). If $kv_0/\Gamma \sim 1$, the excitation is strongly selective with respect to electron direction. The high selectivity becomes especially obvious when $\hbar\omega$ is just slightly less than the gap energy $2|V_G|$ and only electrons moving against the light can be excited, provided that $\hbar\omega + qv \geq 2|V_G|$. To some extent this particular case of selective excitation is similar to that considered in Refs. 2,6 for bulk p-type Ge.

The function $L(\hbar\omega) \propto dR/d\omega$ determines the spectral dependence of the LID current excited in the vicinity of an energy gap. Plots of $R(x)$ and $L(x)$ for various values of $\gamma_0 \equiv \hbar\Gamma$ are presented in Figs. 2(a) and 2(b), respectively. $L(x)$ has a strongly asymmetrical dependence on $x - x_0 \equiv \hbar\omega - 2|V_G|$ and can take on both positive and negative values, suggesting that the current can be directed with or against the light depending on the frequency. $L(x)$ is zero at some small positive $y = x_1 - x_0$ $(y \sim \gamma_0)$; $L(x) > 0$ for $x > x_1$ and $L(x) < 0$ for $x < x_1$. With negative detuning, it is the electrons moving against the light that are the more excited and $L(\omega)$ is negative, and the current flow $\mathbf{J}_{\mathrm{LID}}$ in (33) is directed with $\mathbf{q}$ if $\nu_2 m_2 > \nu_1 m_1$. The opposite occurs for positive detuning (when $x > x_1$).

IV. LID DUE TO INDIRECT ELECTRON TRANSITIONS

For some materials, optical excitation involves indirect (nonvertical) transitions which do not conserve electron momentum. Since light penetrates metals only slightly, so that the radiation probes only a few atomic layers near the surface, there is symmetry breaking which may result in the relaxation of the optical selection rules. In that case, indirect transitions, which do not conserve the projection of momentum normal to the surface, may be important for some interband optical transitions.[32] (However, even for a small light penetration depth, direct transitions can still play the dominant role at certain photon energies. This was shown to be the case in photoemission from Ag films.[32,33]) Indirect optical transitions are particularly important in the case of rough metal films when localized surface plasmon (LSP) excitations are induced in roughness features. This excitation results in local fields with a strong r^{-3} spatial dependence that breaks translational invariance and acts as a continuous source of momentum.[33]

It is clear that the energy interval and the number of states in $\mathbf{k}$ space available for optical excitation are different for electrons moving with and against the light, again due to the Doppler effect. Therefore, one expects that even for indirect surface-assisted transitions LID can be observed.

We use the spectral variable $x = x - x_0 = \hbar\omega - 2|V_G|$. Note that the energy gap $2|V_G|$ can have different values in the vicinity of a surface as compared to the bulk. This possibility can be taken into account by renormalizing $2|V_G|$. In the constant matrix element approximation, the concentration of excited electrons is proportional to the volume of $\mathbf{k}$ space allowed by the energy conservation requirement:

$$\Gamma_2 N_2 = A \int_{[(E_F - X)/\beta]^{1/2}}^{(E_F/\beta)^{1/2}} dk_\perp \int_0^{(E_F/\beta - k_\perp^2)^{1/2}} 2\pi k_\parallel dk_\parallel , \tag{35}$$

where A is a coefficient of proportionality (depending on the matrix element) and $k_\perp$ and $k_\parallel$ are momentum projections normal and parallel to the surface, respectively.

The flux of excited electrons is nonzero when the Doppler effect is taken into account. The Doppler effect modifies the volumes of $\mathbf{k}$ space involved in the excitation of electrons moving with and against the light. Using (14), in the steady-state limit one finds

$$(\Gamma_2 + \nu_2)\mathbf{j}_2 = A\frac{\mathbf{q}}{q} e \int_{[(E_F - X)/\beta]^{1/2}}^{(E_F/\beta)^{1/2}} dk_\perp \left\{ \int_0^{(E_F/\beta - k_\perp^2)^{1/2}} \left(\frac{\hbar}{m} k_q\right) dk_q \int_{-[E_F/\beta - k_\perp^2 - (k_q^2 - 2qk_q)]^{1/2}}^{[E_F/\beta - k_\perp^2 - (k_q^2 - 2qk_q)]^{1/2}} dk_y \right.$$
$$\left. + \int_{-(E_F/\beta - k_\perp^2)^{1/2}}^{0} \left(\frac{\hbar}{m} k_q\right) dk_q \int_{-[E_F/\beta - k_\perp^2 - (k_q^2 + 2q|k_q|)]^{1/2}}^{[E_F/\beta - k_\perp^2 - (k_q^2 + 2q|k_q|)]^{1/2}} dk_y \right\}, \tag{36}$$

where $k_\perp \equiv k_z$ and $k_q \equiv k_x$. Integrating in (35) and (36) using the steady-state equality

$$\Gamma_2 N_2 = \frac{\epsilon'' I}{\hbar c}, \tag{37}$$

one obtains

$$\mathbf{j}_2 = \frac{1}{2}\frac{\mathbf{q}}{q}(ev_F)\frac{qv_F}{E_F/\hbar}\left[\frac{\Gamma_2}{\Gamma_2 + \nu_2}\frac{\epsilon'' I}{\hbar\Gamma_2 c}\right], \tag{38}$$

where the Fermi velocity v_F is defined by $E_F = \frac{1}{2} m v_F^2$.

Using (16) and (38) one ultimately arrives at the following expression for the steady-state current:

$$\mathbf{J}_{\mathrm{LID}}^{(\mathrm{ind})} = \frac{\mathbf{q}}{q}\frac{\nu_1 m_1 - \nu_2 m_2}{2\nu_1 m_1}(ev_F)\frac{qv_F}{E_F/\hbar}\left[\frac{\Gamma_2}{\Gamma_2 + \nu_2}\frac{\epsilon'' I}{\hbar\Gamma_2 c}\right], \tag{39}$$

which suggests that the direction of the electron flow is opposite to the direction of the photon flux when $\nu_2 m_2 > \nu_1 m_1$.

The frequency dependence of LID due to indirect electron transitions is obtained by integrating in (36):

$$\mathbf{J}_{\mathrm{LID}}^{(\mathrm{ind})} \propto \frac{2}{3}E_F^{3/2} - E_F(E_F - X)^{1/2} + \frac{1}{3}(E_F - X)^{3/2}, \tag{40}$$

which becomes

$$\mathbf{J}_{\mathrm{LID}}^{(\mathrm{ind})} \propto (\hbar\omega - 2|V_G|)^2 \tag{41}$$

for excitation near the energy gap. Comparing (33) and (39), we conclude that the selectivity of electron excitation with respect to electron velocity is significantly less for indirect transitions. Accordingly, in the vicinity of the energy gap, LID for direct transitions is larger by a factor $E_F/(\hbar\Gamma)$ than for indirect transitions.

V. LIGHT-INDUCED DIFFUSIVE FLOW OF ELECTRONS

Light-induced diffusive flow (LIDF) of electrons arises when the spatial distribution of the light intensity in the medium is strongly nonuniform. Light penetration in metals is typically a few tens of nm (e.g., for Ag the penetration depth is less than 20 nm at $\lambda = 500$ nm). The intensity changes significantly over this distance, resulting in large light intensity and particle concentration gradients in the upper and lower bands. Large diffusive flows of unexcited and excited electrons would then appear along and opposed to the intensity gradient, respectively. If the electron mobilities in the two bands are different, then a net LIDF electron current, similar to the LID current considered above, will be induced by the light. In many cases the current due to LIDF may significantly exceed that due to LID. Additionally, LIDF can occur in the direction normal to the laser beam since the intensity gradient can be large in this direction. LIDF, like LID, results from the entropy exchange between particles and photons rather than from direct momentum transfer by the light. Note that LIDF is the analog of light-induced pulling in gas kinetics.[14,17]

LIDF results from the spatial gradient $\nabla_{\mathbf{r}}$ term in (2). Multiplying the equation by $\mathbf{v_k}$ and integrating results in (in the steady state)

$$(\Gamma_2 + \nu_2)\mathbf{j}_2 + \frac{1}{3} e v_2^2 \nabla_{\mathbf{r}} N_2(\mathbf{r}) = -(\Gamma_2 + \nu_2)\mathbf{i}, \tag{42}$$

where $\mathbf{i}$ is the current associated with the velocity-selective excitation,

$$\mathbf{i} = -\frac{1}{\Gamma_2 + \nu_2} e \int v_{\mathbf{k}} \sigma(\omega', \mathbf{k}) d\mathbf{k}, \tag{43}$$

and v_2^2 is the average square velocity in the upper band,

$$\int v^2 f_2(\mathbf{k}) d\mathbf{k} \equiv \frac{1}{3} v_2^2 \int f_2(\mathbf{k}) d\mathbf{k} = \frac{1}{3} v_2^2 N_2. \tag{44}$$

According to (16) and (22),

$$\mathbf{i} = \frac{\mathbf{q}}{q} (e v_0) \frac{q v_0}{\Gamma_2 + \nu_2} \left[\frac{I}{\hbar c} \frac{\partial \epsilon''}{\partial \omega} \right], \tag{45}$$

which, in the vicinity of the energy gap, is more specifically given by [see (33)]

$$\mathbf{i} = -\frac{\mathbf{q}}{q} (e v_0) \frac{q v_0}{\Gamma} \left[\frac{\Gamma_2}{\Gamma_2 + \nu_2} \frac{I \epsilon''}{c \hbar \Gamma_2} \right] L(\omega). \tag{46}$$

Using (16), (37), and (42) one ultimately obtains the current

$$\mathbf{J} = -\frac{\nu_1 m_1 - \nu_2 m_2}{\nu_1 m_1} \left\{ \mathbf{i} + e D_2 \frac{\epsilon''}{\hbar \Gamma_2 c} \nabla_{\mathbf{r}} I \right\}, \tag{47}$$

where D_2 is the diffusion coefficient for the electrons in the upper band:

$$D_2 = \frac{1}{3} \frac{v_2^2}{\Gamma_2 + \nu_2}. \tag{48}$$

Thus, there are in general two sources to the net electron current: The first is due to the velocity-selective excitation associated with the Doppler effect (''LID source,'' $\mathbf{i}$) and the second to the nonuniform spatial distribution of excited electrons (''LIDF source,'' $\propto \nabla_{\mathbf{r}} I$). When the light intensity is nonuniformly distributed in the sample both LID and LIDF would occur simultaneously.

VI. ESTIMATES

We will now present some numerical estimates of the magnitude of the LID effect. The crucial parameter is the relative difference in the mobility of the particles, $\mu_i = e/(\nu_i m_i)$, in the two bands [see (22) and (33)]. In general, the difference would be significant because the mass and the particle scattering rate depend strongly on the quantum state. When the lower band of a pure material is filled (as in semiconductors and insulators) the scattering rate in that band is expected to be lower than in the upper band by a factor $E/k_B T \gg 1$.

Within the approximations used thus far, $\Gamma/q v_0$ should be small. However, even for $\Gamma/k v_0 \sim 1$ formula (33) would still provide a good estimate of the magnitude of the effect. In calculating this we will assume that the product $(|\nu m_1 - \nu m_2|/\nu m_1) \times (k v_0/\Gamma) \sim 1$. The function $L(\omega)$ in (33) and (34) is also of the order of unity under optimum conditions (see Fig. 2).

Equation (33) indicates that it is the factor $\Gamma_2 + \nu_2$ in the denominator which will affect the current strongly. To make this parameter small, thereby increasing J_{LID}, one needs to decrease the scattering rate ν_2 by using materials of high purity and, perhaps, by operating at low temperatures; both tend to reduce scattering processes. Note that the relative difference in electron mobility in the two bands remains unchanged when ν_1 and ν_2 are decreased by the same factor. The quantity $\Gamma_2 + \nu_2$ can vary over a wide range from 10^9 s^{-1} ($\nu_2 \leqslant \Gamma_2$) to 10^{13} s^{-1} ($\nu_2 \gg \Gamma_2$) depending on the scattering rate. Thus one concludes that the optimum conditions for LID exist when the absolute value of the scattering rate is low ($\nu_2 \leqslant \Gamma_2$) while the relative values of the particle mobilities in the two bands differ significantly.

Assuming $v_0 \sim 10^8$ cm/s, $\epsilon_0'' \sim 1$, $L(\omega) \sim 1$, $|(\nu_1 m_1 - \nu_2 m_2)/(\nu_1 m_1)| \times q v_0/\Gamma \sim 10^{-1}$, and $(\Gamma_2 + \nu_2) \sim 10^{10} - 10^{14}$ s^{-1}, we estimate the current density (per unit intensity) from (33) to be in the range $J_{\mathrm{LID}}/I \sim 10^{-2} - 10^2$ A/W.

In an open circuit the estimated current density would result in a potential difference $\Delta\phi = lJ/(N_0 e \mu)$ across an illuminated sample of length l, where N_0 is the electron density, in the range $\phi \sim 10^{-8} - 10^{-4}$ V for $I = 1$ W/cm^2 and $l = 1$ cm and for typical values of N_0 and electron mobility $\mu \sim e/m\nu \sim 10^4$ (CGSE). The parameters used are typical of

metals. Since optical depth of metals is of the order of 10^2 Å, the current is expected to be in the range 10^{-8}–10^{-4} A. The predicted magnitude of the effect is large enough that measurable currents are possible even with cw radiation fluxes in the 1 W/cm^2 range.

The resistivity $r \sim (N_0 e \mu)^{-1}$ for semimetals or insulators can be many orders of magnitude larger than for metals. Since the LID current density for various materials is similar in magnitude under optimum conditions, the potential difference across a sample ($\propto r$) can be much larger for materials with low conductivity than for metals (see also Sec. VIII). Consequently, a LID voltage in the range 10^{-2}–10^{-1} V may be obtainable, for example, for semimetals.

VII. EXPERIMENTAL STUDIES OF LID IN METALS

Two experimental observations provide evidence for the existence of LID in metals. They are both based on the comparative photoelectric response between well-annealed Ag films (smooth films) and Ag films deposited onto a low-temperature substrate so that roughness features are generated (rough films). The first observation, although compelling, is indirect. It emerges from the examination of the angle-of-incidence dependence of the *total* photoemission yield from the two types of Ag films. The second observation is more direct, consisting of the detection of an asymmetric angular distribution of photoelectrons excited above the vacuum level of the metal by obliquely incident light. We associate this asymmetry with the asymmetric current flow characteristic of LID.

One-photon and two-photon electron emission from rough and smooth Ag films was previously reported.[34] In one set of measurements a pulsed nitrogen laser operating at 3.7 eV was used to record the one-photon signal. This was done by lowering the work function of the Ag films from their normal values (4.3 eV for smooth and 4.2 eV for rough films) to values below 3.7 eV by exposure to background molecules in the vacuum system. It was found that the photocharge was linearly dependent on the laser pulse power and independent of the degree of focusing of the light on the sample, thereby confirming that the photoemission was a one-photon process. Within the vacuum chamber the photocurrent was detected using a heavily biased wire placed in front of the sample as the collector. The sample could be rotated about the z axis, perpendicular to the horizontal plane, thereby allowing one to record the effect of varying the incidence angle of the exciting laser for s and p polarization. The relative quantum yield Y was recorded as the photoemission current normalized to its value at normal incidence. For a smooth Ag film the data are shown in Fig. 3(a) for both s and p polarization of the incident radiation field. The two lines drawn through the data points of Fig. 3(a) correspond to the radiative absorbance calculated based on the reflectivity (R) data for bulk Ag using known optical constants and the appropriate Fresnel reflectance coefficients. Clearly, the relative quantum yield as a function of incidence angle follows the angular dependence of the absorptivity of the material, $1-R$, calculated for s and p polarization. The smooth Ag film therefore behaves as bulk Ag. This result is further supported by other measurements, especially energy-resolved photoemission measurements on Ag that clearly indicate the predominance of direct (momentum conserving) transitions.[33]

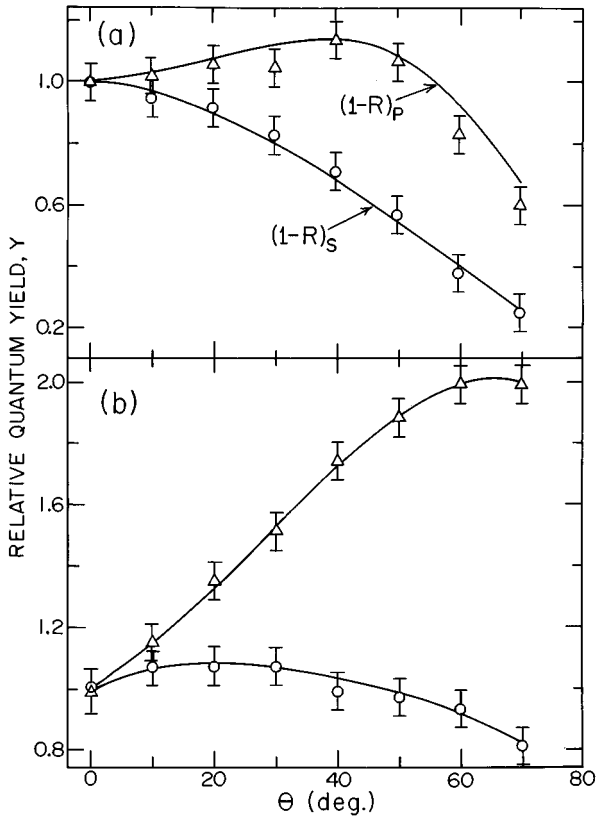

FIG. 3. Relative quantum yields of one-photon photoelectron emission from smooth (a) and rough (b) Ag films as a functions of the angle of incidence, Θ. Open circles are for s-polarized light and open triangles are for p polarization. The lines in (a) are calculated based on the known angular dependence of the reflectivity of Ag. The lines in (b) are guides to the eye. The scale of (a) and (b) are in equivalent units.

In contrast, the angular-of-incidence dependence of the relative quantum yield for a rough, cold-deposited, Ag film [Fig. 3(b)] does not follow the reflectivity behavior seen for smooth Ag films. The data points in Fig. 3(b) cannot be explained on the basis of the $1-R$ curves alone [the lines drawn through the points of Fig. 3(b) are an aid to the eye]. However, it is possible to represent the behavior of the data in Fig. 3(b), with an additional polarization-independent angular factor $f(\theta)$, which differs from unity only for rough Ag films. Thus, photoemission from a smooth film is characterized by $Y_{\text{smooth}} \propto (1-R_{s,p})$ while for a rough Ag surface $Y_{\text{rough}} \propto (1-R_{s,p}) f(\theta)$. The angular factor $f(\theta)$ can be extracted from the ratio $Y_{\text{rough}}/Y_{\text{smooth}} = f(\theta)$. The result is shown in Fig. 4. The function $f(\theta)$ was also extracted from s- and p-polarized two-photon excited photoemission from rough silver surfaces (see below). These values are also presented in Fig. 4.

We believe that LID provides additional channels for electron escape from a rough surface that are not available to a smooth surface. This point is pictorially presented in Fig. 5 where electron escape from a hemispherical surface boss is considered.

The rough surface may be considered to be a collection of a large number of protrusions. An excited electron experi-

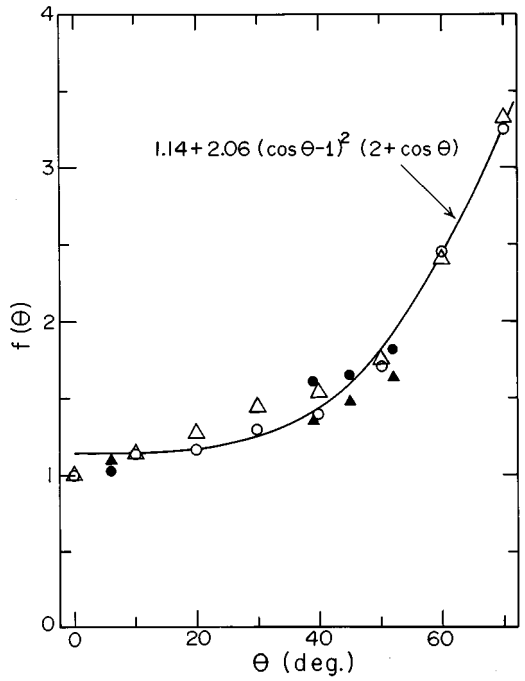

FIG. 4. The angular factor $f(\theta)$. Open circles and triangles refer to one-photon data (s polarization and p polarization, respectively). The solid circles and triangles are derived from two-photon data. The solid line is calculated with Eq. (49) using the values of the parameters indicated in the figure.

ences many quasielastic collisions diffusing to the metal-vacuum interface. LID provides an additional component for delivering excited electrons to a lateral surface of a roughness feature. Despite the fact that the LID macroscopic velocity of excited electrons, $\mathbf{u}_2=\mathbf{j}_2/N_2$, is usually less than the characteristic electron velocity v_0, the time required to deliver a hot electron to the interface by the directed LID process can be less than, or comparable to, that needed to deliver the electron by diffusive motion with its random (and, therefore, long) path. Taking the surface features (naively) to be hemispheres one can determine that only the fraction $p(\theta)=\frac{1}{2}(1-\cos\theta)^2(2+\cos\theta)$ of the total number of electrons set into motion by LID can reach the metal-vacuum interface. Since LID operates in addition to diffusion, the function $f(\theta)$ describing the ''extra'' angle-of-incidence dependence of the photoemission is given by

$$f(\theta)=1+\frac{\kappa}{2}(1-\cos\theta)^2(2+\cos\theta), \tag{49}$$

where κ is a measure of the ratio of rate with which a hot electron reaches the surface by LID over the diffusion rate. The data shown in Fig. 4 (points) were fit to a modified version of (49). Since the data contain an experimental error, it was thought more correct to allow the $\theta=0$ intercept to be an adjustable parameter rather than forcing it to have an error-free value of unity. The line in Fig. 4 is the result of this two-parameter fit, yielding 1.14 for the $\theta=0$ intercept and 2.06 for the value of $\kappa/2$. The fit is quite good. Recently, we have imaged the roughness features of cold-deposited Ag films with scanning tunneling microscopy. The size distribution of the surface features is very broad and modeling a complex surface with hemispheres is simplistic; however, the good fit of formula (49) indicates that the essential physics is likely robust.

It is clear that for a flat surface the LID of excited electrons with $\mathbf{j}_2$ parallel to the wave vector of the light obliquely incident to the surface cannot deliver electrons to the metal-vacuum interface and, accordingly, would not contribute noticeably to the photoemission if $u_2 \ll v_0$. However, at frequencies for which $\mathbf{j}_2$ is directed against the wave vector the delivery of hot electrons to the interface by LID could be important despite the condition $u_2 \ll v_0$. This is because the random path characterizing electron diffusion is much longer than the path associated with LID and, accordingly, for electrons well below the surface, LID can become an important mechanism in photoemission. This implies that for a smooth surface and $u_2 \ll v_0$ LID can contribute significantly to photoemission only if $\mathbf{u}_2$ is directed against the light, while for a rough film, which has features with a lateral surface, LID can contribute to electron escape for any relative direction of $\mathbf{u}_2$ and $\mathbf{q}$. In our experiments the laser frequencies were used such that the flow of hot electrons $\mathbf{j}_2$ was parallel to the wave vector and, therefore, LID of hot electrons could contribute to the photoemission from rough films only. [The resultant current flow $\mathbf{J}_{\mathrm{LID}}=\mathbf{j}_2(\nu_1 m_1-\nu_2 m_2)/\nu_1 m_1$ is against $\mathbf{j}_2$ if $\nu_2 m_2>\nu_1 m_1$; however, the photoemission probes the current of excited electrons only.]

To obtain the direction-varying LID, a tunable laser source, with photon energy close to the energy gap must be applied.

Angle-resolved photoemission measurements were also performed on clean surfaces prepared by vacuum deposition of Ag under UHV conditions (10^{-10} Torr). Rough films gave easily measurable photocurrents that depended quadratically on the laser pulse power and inversely on the focal point area of the radiation: This is entirely consistent with a two-photon

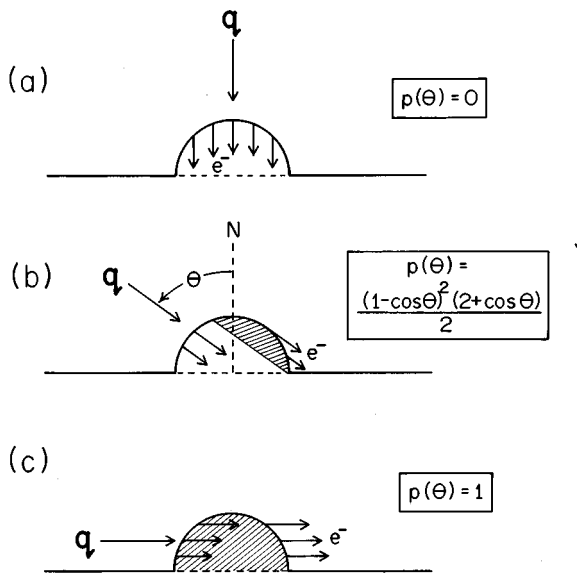

FIG. 5. The volume fraction of a semispherical protrusion from which electrons moving along the wave vector can reach the metal-vacuum interface.

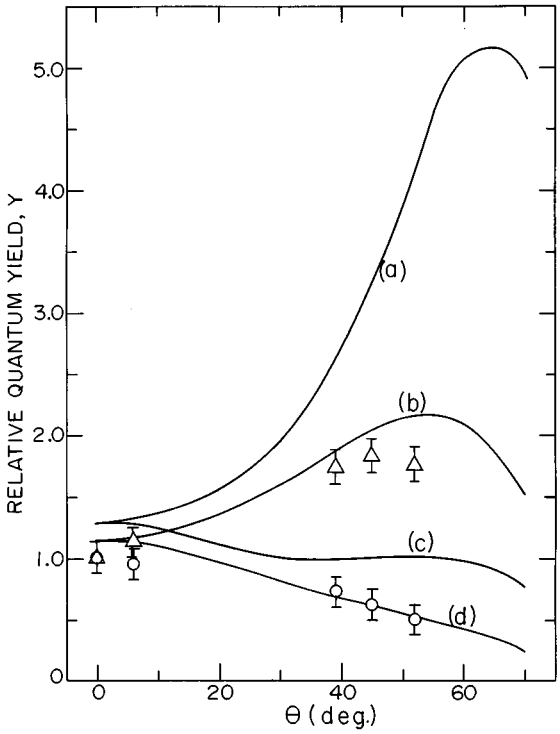

FIG. 6. Two-photon relative quantum yields for a rough film as a function of incidence angle. The calculated solid lines are as follows: (a) $[(1-R_p)f(\theta)]^2$, (b) $(1-R_p)^2 f(\theta)$, (c) $[(1-R_s)f(\theta)]^2$, (d) $(1-R_s)^2 f(\theta)$.

process. There was insufficient signal to record a quadratic photoelectric response from smooth films. This is now understood to be due to the large photoemission enhancement in rough films associated with localized surface plasmon excitation.[33] Thus, we were not able to calculate $f(\theta)$ from data collected solely with two-photon excitation. However, if we suppose that the $f(\theta)$ factor is associated with the escape of the electron from the surface, and is not related to the absorption process, then one would expect the angular variation of Y for two-photon excitation to be of the form $Y_{\text{rough}} \propto (1-R_{s,p})^2 f(\theta)$. Figure 6 shows that this is the case. Curves (b) and (d) fit the data points best, while $[(1-R_{s,p})f(\theta)]^2$ does not, vindicating our assumption. The two-photon values of $f(\theta)$ were calculated from the points given in Fig. 6 but with $(1-R)$ values derived from the one-photon measurements. The two-photon values are included in Fig. 4 as the solid circles and triangles. They are seen to lie on the same curve as the one-photon data. The independence of $f(\theta)$ from polarization argues strongly for a dependence on wave vector rather than field as required by LID.

In a second experiment involving LID (Fig. 7), radiation from a XeCl excimer laser exits the laser cavity as a rectangular beam about 1 cm $\times$ 2 cm. The most uniform central portion of the beam is selected by a circular iris diaphragm (I), resulting in a circular beam (about 0.75 cm diameter) which is split into two paths A and B passing through independent attenuation (A), polarization selection (P), and focusing (L) optics and impinging on a common spot on the sample substrate (S) situated inside an ultrahigh-vacuum

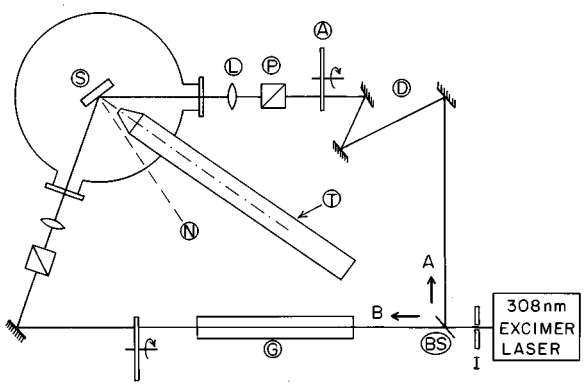

FIG. 7. Experimental arrangement for the detection of asymmetric photoemission from Ag films. The symbols are as follows: S, surface housed in the UHV chamber; N, surface normal; T, time-of-flight tube; L, lens; P, linear polarizer; A, variable neutral density filter or attenuator; D, delay line; G, glass tube; BS, beam splitter; I, iris diaphragm. The two paths beyond BS are labeled A and B.

chamber. The two beams strike the surface with equal angles of incidence (55°) symmetrically about the surface normal. A silver film is deposited from an effusive source at an approximate rate of 1 nm/s. Deposition can be carried out either on a room temperature substrate, in which case smooth, annealed Ag films are formed, or with the substrate cooled to as low as 30 K, in which case rough, unannealed films form. Film deposition was complete after several minutes, much shorter than the time required to contaminate the surface significantly (pressure 5×10^{-11} Torr).

The laser light induces two-photon electron emission from the silver surface. A narrow solid angle of the forward electron intensity distribution is collected through a 1 m, magnetically shielded time-of-flight tube (T) and detected on a 2 cm diameter microchannel plate (about 10^{-4} sr are subtended by the detector). The electron kinetic energy distribution is accumulated on a pulse-to-pulse basis with each laser pulse contributing a few electron counts so as to maintain a relatively low space charge in order to reduce broadening. Although the two laser paths are symmetrically oriented with respect to the surface normal, the time-of-flight electron analyzer is asymmetrically placed at 20° on one side of the normal, as shown in Fig. 7. The system is, therefore, sensitive to a possible asymmetry in the spatial distribution of the photoemission.

The two laser paths A and B are made equal in length to within 1 cm over a total length of 2.5 m by using a delay line (D). The two laser beam paths are p polarized with respect to the surface by adjusting the rotational orientation of two high extinction Glan-Thompson linear polarizers. Two matched lenses then focus the light beams onto the sample. The convergence, and subsequent divergence of the two light paths after reflection from the surface, imparted to the light by the lenses allows one to observe the two light beams independently at any point along the light path. In this way the two beams can be aligned so that they counterpropagate precisely over a path length several meters in length. Thus, the degree of spatial overlap of the two beams at the surface is very high.

In order to ensure reasonably tight focusing of the laser

light on the surface we used the shortest focal length lenses which were placed just outside the vacuum windows of the chamber. Laser power measurements were made along the beam paths and adjusted to be approximately equal. Fine tuning of the laser power during the experiment was performed by recording the total electron recharge current from the films. A collector was placed inside the vacuum chamber and biased to +300 V. The total recharge current per pulse was than passed through a fast preamplifier and processed with a digital oscilloscope. The two attenuators were adjusted such that the total recharge current measured with beam A was exactly equal to that of beam B. With both beams A and B on, the total electron recharge current was found to be double in all cases. Although we are measuring a two-photon process, a factor of 2 (rather than 4) was observed because the temporal coherence is much shorter than the pulse duration of the laser. (Although we do not know the detailed mode structure of our laser, an approximate analysis based on the reported energy width indicates that temporal phase coherence would be difficult to achieve.) In order to eliminate the possibility that our observations are a trivial result of interference, measurements were made by purposely disturbing any possible coherence that might exist. The two paths A and B in Fig. 7 are effectively the two arms of Mach-Zener interferometer. A glass tube (G) was placed along one path (B) and heated. The resulting change in refractive index in the hot air within the tube would have changed the coherence conditions strongly, yet the photoemission results were unaltered.

Two films, a smooth one and a rough one, were generated as 5 mm diameter circular spots one above the other, on the same substrate. The height of the substrate in the ultrahigh-vacuum chamber can be adjusted externally so that the photoemission spectra of the two films can be recorded in turn.

Figure 8 shows the two-photon photoemission spectrum for smooth and rough silver films. For the smooth films the photoemission spectra recorded alternately with the two light ray directions have a similar spectral distribution and total integrated intensity. Contrariwise, for the rough films the total intensity of the photoemission spectra differed by over a factor of 2 according to the direction of illumination. The photoemission was found to be greater in the direction of the wave vector of the light. This is consistent with (16) and (28), (29) which suggest that the direction of the flow of the excited electrons coincides with the direction of the wave vector when the total photon energy $2\hbar\omega = 8$ eV.

The possibility that the effect was a result of an asymmetry of the roughness features themselves with respect to the metal surface normal was eliminated by purposely producing films with spatially asymmetrical surface features by depositing silver obliquely on the cooled substrate at an angle of 45°. The photoemission asymmetry was shown not to depend significantly on the mode of preparation of the surface. The results reported in Figs. 3 and 6 are from surfaces grown such that the direction deposition lay along the surface normal.

One should point out in passing that the experimental setup intrinsically breaks symmetry with respect to the surface normal so that even in the absence of LID, asymmetric photoemission might be possible. In that case, the inequivalence should be brought about by the asymmetry in the direction of the electric vector rather than the wave vector of the light with respect to the surface normal. There should, therefore, be no reason why smooth as well as rough surfaces should not manifest photoemission asymmetry. Even if one postulates that, for some reason, rough surfaces amplify the asymmetry of the two-photon photoemission, it would be difficult to reconcile this with the observed insensitivity to the direction of the orientation of the roughness features with respect to the photoemission detector axis. Nor would the angle of incidence effect on the total photoyield reported in Refs. 27,34 be explicable under that assumption.

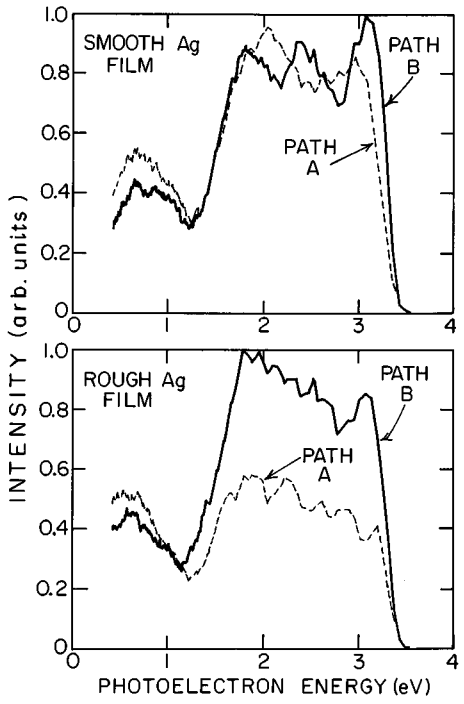

FIG. 8. Energy-resolved photoelectron spectra from smooth and rough films of Ag. The spectra are labeled according to the direction of propagation of the light as in Fig. 7.

We conclude, therefore, that the observed asymmetry in the angular distribution of photoelectrons is a strong indication of the LID of hot electrons.

VIII. DISCUSSION AND SUMMARY

Light-induced kinetic effects in solids exist as a result of the combination of momentum-selective excitation with state-dependent scattering of carriers from impurities, phonons, excitons, etc. These effects result from entropy transfer between photons and particles, that is, from the transfer of order from photons to particles, rather than from radiation pressure. (This sort of light-matter interaction based on entropy transfer probably plays a role in other systems as well. In particular, it provides a plausible explanation of some phenomena in astrophysics, such as the D/H distribution in the Universe.[35])

The light-induced kinetic effects considered here manifest themselves as induced currents and/or potential differences in solids when a sample is irradiated by light. Particles (electrons and/or holes) with momentum components directed

along and opposite to the wave vector of the exciting light beam are shown to be inequivalently absorbed due to the Doppler effect. This results in a light-induced carrier drift that leads to an overall current in the sample provided the particle translational relaxation is internal state dependent.

LID accompanying momentum nonconserving transitions was shown also to exist due to the slight difference in the volumes of **k** space available to excited electrons moving with and against the light [see (39)]. The selectivity of the excitation is lower in this case compared to the case of direct electron transitions which conserve electron momentum and, accordingly, the effect is also smaller.

Light-induced diffusive flow (LIDF) of carriers resulting from the nonuniform spatial distribution of the light intensity in the sample was also considered. In particular, the effect of the strong attenuation of the radiation in metals where the light penetration is only a few tens of nm was explored. The intensity gradient leads to a nonuniform spatial distribution of excited electrons resulting, in turn, in large counterpropagating diffusive flows of excited electrons and holes. If the mobilities of the electrons and the holes are different, then a resultant LIDF occurs. Formula describing both effects simultaneously the LID and LIDF is derived [see (47)].

The strong gradients of electrons and holes due to both LID and LIDF result in the formation of a double layer of carriers in a thin metal film. To some extent this system can be viewed as a light-induced *p-n* junction. In a steady state the two currents associated with LID and LIDF are compensated by a current due to the light-induced voltage. An attractive feature of this pseudo ''*p-n* junction'' in metals is the fact that it can be controlled by light.

It is also worth noting that the simultaneous initiation of the large particle gradients and LID and/or LIDF currents can result in very interesting and complex electron dynamics. In particular, both longitudinal and transverse potential differences can be induced simultaneously. Vortex currents are anticipated and chaotic electron dynamics may result under some conditions.

The majority of the conclusions reached in the present treatment are valid for a range of materials. In particular, effects due to interband optical transitions can occur in semimetals, semiconductors, and insulators. The potential difference in an open circuit due to LID is given by $\Delta\phi = lJ/(N_0 e\mu)$ [see (17)], which is proportional to the sample resistivity, $r \sim (N_0 e\mu)^{-1}$ (N_0 and μ are the conduction electron concentration and the particle effective mobility, respectively). The LID current in this case is compensated by the current due to the induced electrostatic potential difference resulting from the nonuniform charge displacement in the sample. Since $\Delta\phi \propto r$, the light-induced voltage increases for materials with high resistivity; hence, under the right circumstances, solids with low conductivity, such as semimetals, semiconductors, and insulators, are more appropriate candidates than metals for the observation of these effects. The key point is that the LID current depends on the number of selectively excited particles rather than on the total number of conduction electrons. Therefore, in materials with low conductivity, it can be, in principle, as large as in metals while at the same time the resulting potential difference can be much larger. A necessary condition for LID is the existence of strong and momentum-selective optical excitations.

Our experimental observation of the spatially asymmetric photoemission from rough silver film is interpreted to be an indirect manifestation of the LID. The observed dependence of the photoemission yield on the angle of the incident light is successfully explained in terms of LID.

The spatial asymmetry of the photoelectrons suggests that the photoelectrons leaving the surface possess a nonzero total momentum. Accordingly, the same should be true regarding the electrons remaining inside the sample. Thus, asymmetrical photoemission is anticipated to result in a net current of the carriers left behind in the sample. This effect can occur even if the mobilities of the electrons in the two bands are identical, i.e., $\nu_1 m_1 = \nu_2 m_2$.

ACKNOWLEDGMENTS

The authors are grateful to NSERC and CEMAID for financial support.

*Present address: Dept. of Chemistry, University of Washington, Seattle, Washington 98195.

[1] A. A. Grinberg, E. D. Belorusets, and E. Z. Immanov, Fiz. Tekh. Poluprovodn. **5**, 2010 (1971) [Sov. Phys. Semicond. **5**, 1748 (1972)]; Anatoly Grinberg, *The Discovery of the Photon-Drag Effect* (Delphic Associates, Falls Church, VA, 1986).

[2] A. A. Grinberg and L. V. Udod, Fiz. Tekh. Poluprovodn. **8**, 1012 (1974) [Sov. Phys. Semicond. **8**, 658 (1974)].

[3] A. A. Grinberg and S. Luryi, Phys. Rev. Lett. **67**, 156 (1991).

[4] A. M. Dykhne, V. A. Roslyakov, and A. N. Starostin, Dokl. Akad. Nauk SSSR **254**, 599 (1980) [Sov. Phys. Dokl. **25**, 741 (1980)].

[5] S. Luryi, Phys. Rev. Lett. **58**, 2263 (1987).

[6] A. A. Grinberg and S. Luryi, Phys. Rev. **38**, 87 (1988).

[7] M. I. Stockman, L. N. Pandey, and T. F. George, Phys. Rev. Lett. **65**, 3433 (1990).

[8] A. D. Weick, H. Sigg, and K. Ploog, Phys. Rev. Lett. **64**, 463 (1990).

[9] E. M. Skok and A. M. Shalagin, Pis'ma Zh. Éksp. Teor. Fiz. **32**, 201 (1980) [JETP Lett. **32**, 184 (1980)].

[10] A. V. Kravchenko, A. M. Pakin, V. N. Sozinov, and O. A. Shegai, Pis'ma Zh. Éksp. Teor. Fiz. **38**, 328 (1983) [JETP Lett. **38**, 393 (1983)].

[11] L. E. Gurevich and A. Ya. Vinnikov, Fiz. Tverd. Tela **15**, 87 (1973) [Sov. Phys. Solid State **15**, 58 (1973)].

[12] F. Kh. Gel'mukhanov and A. M. Shalagin, Pis'ma Zh. Éksp. Teor. Fiz. **29**, 773 (1979) [JETP Lett. **29**, 711 (1979)].

[13] V. D. Antsygin, S. N. Atutov, F. Kh. Gel'mukhanov, G. G. Telegin, and A. M. Shalagin, Pis'ma Zh. Éksp. Teor. Fiz. **30**, 262 (1979) [JETP Lett. **30**, 243 (1979)].

[14] F. Kh. Gel'mukhanov and A. M. Shalagin, Zh. Éksp. Teor. Fiz. **78**, 1674 (1980) [Sov. Phys. JETP **51**, 839 (1980)]; F. Kh. Gel'mukhanov, L. V. Il'ichov, and A. M. Shalagin, Physica A **137**, 502 (1986); J. Phys. A **19**, 2201 (1986); F. Kh. Gel'mukhanov and L. V. Il'ichov, Chem. Phys. Lett. **98**, 349 (1983); Opt. Commun. **53**, 381 (1985); F. Kh. Gel'mukhanov, Sov. Phys. Dokl., **29**, 45 (1984); Sov. J. Quantum Electron. **14**, 347 (1984).

[15] G. Nienhuis, Phys. Rev. A **40**, 269 (1989); S. J. van Enk and G. Nienhuis, *ibid.* **41**, 3757 (1990); **42**, 3079 (1990); **44**, 7615 (1991).

[16] A. V. Ghiner, Opt. Commun. **41**, 27 (1982); A. V. Ghiner, K. P. Komarov, and K. G. Folin, Zh. Éksp. Teor. Fiz. **82**, 1853 (1982) [Sov. Phys. JETP **55**, 1068 (1982)]; A. V. Ghiner, M. I. Stockman, and M. A. Vaksman, Phys. Lett. A **96**, 79 (1983); M. A. Vaksman, Phys. Rev. B **52**, 2179 (1995).

[17] H. G. C. Werij, J. P. Woerdman, J. J. M. Beenakker, and I. Kucser, Phys. Rev. Lett. **52**, 2237 (1984); P. R. Berman, J. E. M. Haverkort, and J. P. Woerdman, Phys. Rev. A **34**, 4647 (1986).

[18] L. J. F. Hermans, Int. Rev. Phys. Chem. **11**, 289 (1992); R. W. M. Hoogeveen, and L. J. F. Hermans, Phys. Rev. Lett. **65**, 1563 (1990); Phys. Rev. A **43**, 6135 (1991); R. W. M. Hoogeveen, L. J. F. Hermans, V. D. Borman, and S. Yu. Krylov, *ibid.* **42**, 6480 (1990); R. W. M. Hoogeveen, G. J. van der Meer, and L. J. F. Hermans, *ibid.* **42**, 6471 (1990); R. W. M. Hoogeveen, R. J. C. Spreeuw, and L. J. F. Hermans, Phys. Rev. Lett. **59**, 447 (1987); G. J. van der Meer, R. W. M. Hoogeveen, L. J. F. Hermans, and P. L. Chapovsky, Phys. Rev. A **39**, 5237 (1989); G. J. van der Meer, J. Smeets, S. P. Pod'yachev, and L. J. F. Hermans, *ibid.* **45**, 1303 (1992).

[19] P. L. Chapovsky, Phys. Rev. A **43**, 3624 (1991); P. L. Chapovsky, A. M. Shalagin, V. N. Panfilov, and V. P. Strunin, Opt. Commun. **40**, 129 (1981); P. L. Chapovsky, G. J. van der Meer, J. Smeets, and L. J. F. Hermans, Phys. Rev. A **45**, 8011 (1992).

[20] A. K. Popov, A. M. Shalagin, V. M. Shalaev, and V. Z. Yakhnin, Zh. Éksp. Teor. Fiz. **80**, 2175 (1981) [Sov. Phys. JETP **53**, 1134 (1981)]; Sov. Opt. Spectrosc. **50**, 327 (1981); Appl. Phys. **25**, 347 (1981).

[21] A. K. Popov, V. M. Shalaev, and V. Z. Yakhnin, Zh. Éksp. Teor. Fiz. **82**, 725 (1982) [Sov. Phys. JETP **55**, 431 (1982)].

[22] A. K. Popov, V. M. Shalaev, and V. Z. Yakhnin, Z. Phys. D **8**, 367 (1988).

[23] V. M. Shalaev and V. Z. Yakhnin, J. Phys. B **20**, 2733 (1987); Sov. Phys. JETP **60**, 693 (1984).

[24] A. A. Grinberg, D. S. Bulianitsa, and E. Z. Imamov, Fiz. Tekh. Poluprovodn. **7**, 45 (1973) [Sov. Phys. Semicond. **7**, 29 (1973)].

[25] V. G. Agafonov, P. M. Valov, B. S. Ryvkin, and I. D. Yaroshetskii, Fiz. Tekh. Poluprovodn. **6**, 2219 (1972) [Sov. Phys. Semicond. **6**, 1868 (1973)].

[26] M. I. Stockman, L. N. Pandey, and T. F. George, Phys. Rev. Lett. **67**, 157 (1991).

[27] V. M. Shalaev, C. Douketis, and M. Moskovits, Phys. Lett. A **169**, 205 (1992).

[28] Ole Keller, Phys. Rev. B **48**, 4786 (1993).

[29] V. L. Gurevich, R. Laiho, and A. V. Laskul, Phys. Rev. Lett. **69**, 180 (1992).

[30] V. L. Gurevich and R. Laiho, Phys. Rev. B **48**, 8307 (1993).

[31] N. F. Mott and H. Jones, *The Theory of the Properties of Metals and Alloys* (Dover, New York, 1958), p. 64.

[32] R. Y. Koyama and N. V. Smith, Phys. Rev. B **2**, 3049 (1970); N. V. Smith, *ibid.* **3**, 1862 (1971).

[33] C. Douketis, T. L. Haslett, J. T. Stuckless, M. Moskovits, and V. M. Shalaev, Surf. Sci. Lett. **297**, L84 (1993); V. M. Shalaev, C. Douketis, T. L. Haslett, T. Stuckless, and M. Moskovits, Phys. Rev. B **53**, 15 (1996).

[34] T. Stuckless and M. Moskovits, Proc. SPIE **10**, 124 (1989).

[35] S. N. Atutov and A. M. Shalagin, Pis'ma Astron. Zh. **14**, 664 (1988) [Sov. Astron. Lett. **14**, 284 (1988)]; H. I. Bloemink, J. M. Boon-Engering, E. R. Eliel, and L. J. F. Hermans, Phys. Rev. Lett. **70**, 742 (1993).